

The origin of discrete multiple stellar populations in globular clusters

K. Bekki,¹ T. Jeřábková^{2,3}, and P. Kroupa^{2,3}

¹*ICRAR M468 The University of Western Australia 35 Stirling Hwy, Crawley Western Australia 6009, Australia*

²*Astronomical Institute, Charles University in Prague, V Holešovičkách 2, CZ, 180-180 00 Praha 8, Czech Republic*

³*Helmholtz Institut für Strahlen Kernphysik, Universität Bonn, Nussallee 14-16, 53115 Bonn, Germany*

Accepted, Received 2005 February 20; in original form

ABSTRACT

Recent observations have revealed that at least several old globular clusters (GCs) in the Galaxy have discrete distributions of stars along the Mg-Al anti-correlation. In order to discuss this recent observation, we construct a new one-zone GC formation model in which the maximum stellar mass (m_{\max}) in the initial mass function (IMF) of stars in a forming GC depends on the star formation rate (SFR), as deduced from independent observations. We investigate the star formation histories of forming GCs. The principal results are as follows. About 30 Myr after the formation of the first generation (1G) of stars within a particular GC, new stars can be formed from ejecta from asymptotic giant branch (AGB) stars of 1G. However, the formation of this second generation (2G) of stars can last only for [10–20] Myr, because the most massive SNe of 2G expel all of the remaining gas. The third generation (3G) of stars are then formed from AGB ejecta \approx 30 Myr after the truncation of 2G star formation. This cycle of star formation followed by its truncation by SNe can continue until all AGB ejecta is removed from the GC by some physical process. Thus, it is inevitable that GCs have discrete multiple stellar populations in the [Mg/Fe]–[Al/Fe] diagram. Our model predicts that low-mass GCs are unlikely to have discrete multiple stellar populations, and young massive clusters may not have massive OB stars owing to low m_{\max} ($< [20 - 30]M_{\odot}$) during the secondary star formation.

Key words: galaxies: star clusters– globular clusters:general – stars:formation

1 INTRODUCTION

Old globular clusters (GCs) in the Galaxy are observed to have anti-correlations between chemical abundances of light elements (e.g., Carretta et al. 2009, C09; Cratton et al. 2012; Renzini et al. 2015). Since such anti-correlations are seen in almost all of GCs that have been investigated so far, they are now considered to be essential characteristics of GCs. Stars with highly enhanced [Na/Fe] (or [Al/Fe]) and severely depleted low [O/Fe] (or [Mg/Fe]) along the Na-O anti-correlation are often assumed to be formed from gas ejected from previous generations of stars, whereas those with [Na/Fe] and [O/Fe] similar to those of the Galactic halo stars are assumed to be formed from pristine gas within GC-forming molecular clouds. The origin of the anti-correlations has been discussed by several authors in the context of GC formation processes (e.g., Fenner et al. 2004; Bekki et al. 2007, B07; Prantzo & Charbonnel 2006, PC06; D’Ercole et al. 2010, D10, Ventura et al. 2016; Bekki 2017a, B17a). For example, the number fraction of “polluted” stars with high

[Na/Fe] ([Al/Fe]) and low [O/Fe] ([Mg/Fe]) in a GC has been used to provide fossil information on the original mass the GC and the initial mass function of stars in the early phase of the GC formation (e.g., Smith & Norris 1982; D’Antona & Caloi 2004; Bekki & Norris 2006; PC06). Previous theoretical studies of GC formation tried to explain the apparently continuous distribution of stars along the anti-correlation between light element by assuming dilution of AGB ejecta with pristine gas (e.g., B07; D10).

Although the distributions of stars along the anti-correlations were assumed to be continuous in previous observational and theoretical studies of GCs, more precise spectroscopic measurements of chemical abundances of GC stars by Carretta (2014; C14) have recently revealed that (i) the distribution of stars along the [Mg/Fe]–[Al/Fe] anti-correlation in NGC 2808 is not continuous and (ii) there are three distinct groups each of which has different [Mg/Fe] and [Al/Fe]. Such discrete three stellar populations have been also found in NGC 6752 (Carretta et al. 2012; Milone et al. 2013), though they are less clear in comparison with NGC

2808. Marino et al. (2011) also found two distinct groups each of which clearly shows the Na-O anti-correlation in the [Na/Fe]-[O/Fe] diagram for M22. If the presence of discrete multiple stellar populations along the anti-correlations between light elements is a universal feature in old GCs, then it can give a strong constraint on the theory of GC formation. The discrete stellar populations in GCs would imply that such GCs experienced a number of discrete star formation episodes in their early formation histories.

The origin of these new observational results on the discrete multiple stellar populations of GCs, however, have not been discussed so extensively in theoretical studies of GC formation. Renzini et al. (2015) pointed out that the observed discreteness can not be explained by a GC formation scenario in which later generations of stars are formed from ejecta from fast rotating massive stars (FRMS) and massive interacting binaries. Accordingly, the discrete multiple populations in GCs could possibly give strong constraints on the formation processes of GCs. Using new hydrodynamical simulations of GC formation from fractal molecular clouds, Bekki (2017b, B17b) have recently shown that forming GCs can have a number of bursty star formation events in their early (< 300 Myr) evolution. However, such a result is due largely to the adopted model in which ejection of gas from AGB stars can occur only at five separate times (not continuously) for some numerical reasons. Therefore, it remains unclear how forming GCs can have discrete multiple stellar populations.

D’Antona et al. (2016) discussed the origin of at least five discrete populations in NGC 2808 by assuming (i) several distinct episodes of star formation, (ii) gas fueling from AGB stars with different masses (thus different yields), and (iii) dilution of the AGB ejecta with pristine gas. They have shown that the first population (25% of the GC) enriched in N yet not so enriched in He and Na can be formed from gas from lower mass AGB stars diluted by pristine gas. They also have demonstrated that NGC 2808 has a minor population that was chemically polluted by iron-rich ejecta from SNIa. However, they did not discuss the physical basis for the assumed several episodes of star formation in a quantitative manner. They did not provide the physical reasons for the assumed no SNII in 2G populations of GCs either. Thus, it is still theoretically unclear how discrete multiple stellar populations can be formed in GCs.

If the IMF in secondary star formation from AGB ejecta is an invariant canonical one, then the star formation can be truncated by SNe of massive stars only 3×10^6 yr after its commencement, because such SN explosions can easily expel all of the remaining gas within GCs (D’Ercole et al. 2008, D08; D10; B17b). Therefore, a canonical IMF can be a potentially serious problem in the AGB scenario. A way to avoid this problem is to adopt a non-standard IMF in which the upper mass cut-off (m_u) of the IMF is less than $9M_\odot$ (i.e., virtually no SNe) in the formation of later generations of stars from AGB ejecta. However, it is totally unclear how such an apparently unusual IMF is possible during GC formation. Also no previous theoretical studies of GC formation have ever discussed whether and how the observed discrete multiple stellar populations can be achieved in GC formation with a non-standard IMF.

The purpose of this paper is thus to investigate the origin of discrete multiple stellar populations in GCs in the

Table 1. Physical meanings of acronyms and model parameters.

Acronym	Physical meaning
1G	First generation of stars formed from original gas
2G	Second generation of stars formed from ejecta from 1G
3G	Third generation of stars formed from ejecta from 1G
n G	n th generation of stars formed from ejecta from 1G
LG	Later generation of stars formed from AGB ejecta
Δt_{sf}	Duration of star formation (SF) episode
Δt_{tr}	Duration of SF truncation (no SF)
m_{max}	The maximum stellar mass in each SF episode
MC	Molecular cloud forming a GC
M_{mc}	The initial mass of a MC
M_{g}	The total mass of gas
$M_{1\text{G}}$	The total mass of 1G stars
M_{LG}	The total mass of LG stars
\dot{M}_{inf}	The gas infall rate onto the core of a MC
\dot{M}_{agb}	The gas ejection rate of AGB stars
$m_{\text{agb},l}$	The lowest mass of AGB stars for LG formation
SFR	Star formation rate
IGIMF	Integrated galactic initial mass function

context of a non-universal IMF, by assuming that the later stellar generations form in smaller clusters and star formation is interrupted by SN II in the later generations. To describe clustered star formation, we use empirically motivated physical and mathematical formalism of the IGIMF theory (Kroupa et al. 2013). We emphasise that the IGIMF theory is applied here without adjustments for this GC case. The results achieved are therefore not fine-tuned to reach an aim. We particularly investigate the star formation histories of GCs over ≈ 400 Myr using a new GC formation model that incorporates a non-universal IMF self-consistently. A growing number of observational and theoretical studies have recently discussed that the IMF in GC formation can be non-universal using the observed different properties of GCs (e.g., D’Antona & Caloi 2004; Bekki & Norris 2006; PC06; Marks et al. 2012). For example, Marks et al. (2012) have recently estimated the IMF slope for high-mass stars (i.e., α_3 in the Kroupa IMF; Kroupa 2001) for each GC in the Galaxy using the observed mass density of the GC and found that α_3 was quite different between different GCs. Accordingly, it is quite important and timely for the present study to investigate GC formation based on a non-universal IMF.

The structure of the paper is as follows. We describe the new one-zone models of GC formation in §2. We present the results on the star formation histories of forming GCs for different representative models in §3. We describe the possible spreads of [Mg/Fe] and [Al/Fe] of GC stars based on the models in §4. We also discuss the origin of the observed discrete multiple stellar populations of the Galactic GCs based on the present results in §4. We provide important implications of the present results in terms of the origin of multiple stellar populations in GCs in this section in §4. We summarize our conclusions in §5. Although several authors have recently discussed a number of new physical processes related to the origin of multiple stellar populations of GCs, such as merging of GCs (Bekki & Yong 2012; Bekki & Tsujimoto 2016), stripping of stellar envelopes in massive stars (e.g., Elmegreen 2017), gas accretion onto pre-main sequence stars (e.g., PC06), and Bondi-accretion of interstellar medium onto GCs (e.g., Pflamm-Altenburg & Kroupa 2009), we do not discuss them extensively in the present study. We

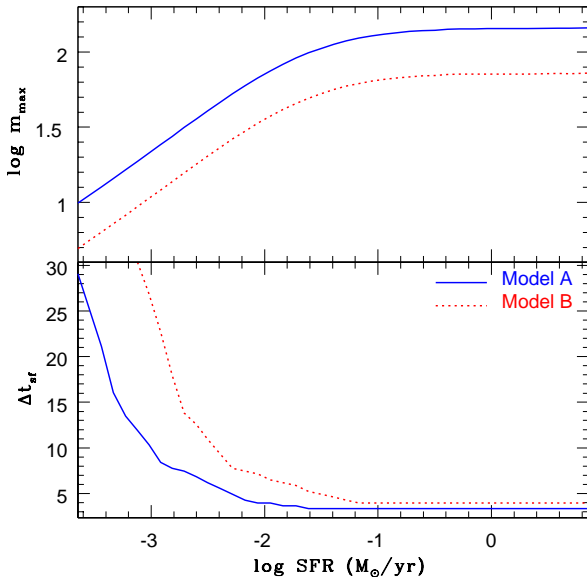


Figure 1. $SFR - m_{\max}$ (upper panel) and $SFR - \Delta t_{\text{sf}}$ relation (lower panel) derived from two IMF models, model A (blue solid) and B (red dotted). Here m_{\max} and Δt_{sf} represent the maximum mass of stars and the duration of star formation in each star formation episode, and it corresponds to the lifetime of the most massive star formed, respectively. The two relations in model A are derived from the IGIMF theory recently developed by several authors, e.g., Kroupa & Weidner (2003), Kroupa et al. (2013), Weidner et al. (2013), and Yan et al. (2017) based on observational results. In model B, the relations are a slightly modified version of the relations in model A: m_{\max} at a given SFR in model B is by a factor of two smaller than that in model A. The details of model A and B are given in the main text.

do not discuss all of the AGB scenario (e.g., the yields, the mass-budget, the dilution problems etc), instead, focus only on the discrete populations in the present paper.

2 THE GC FORMATION MODEL

We here adopt the “AGB pollution scenario” in which later generations (LG) of stars can be formed from gas ejected from AGB stars having evolved from intermediate-mass first generation (1G) stars formed within a GC-forming molecular cloud (MC). We use the term “1G” and “LG” rather than “FG” and “SG” to represent the first and later generations of stars of the GC in the present study, because not just second or third (2G and 3G, respectively), but fourth and fifth generations (4G and 5G) of stars can be formed in the present GC formation models. Table 1 describes the physical meaning of these acronyms used in the present study. Also we focus exclusively on this scenario, though other GC formation scenarios based on chemical pollution by stars other than AGB stars (e.g., FRMSs; Decressin et al. 2007) are possible. These scenarios, however, can not simply explain the discrete multiple stellar populations (e.g., Renzini et al. 2015).

Table 2. Physical parameters for the representative 11 models.

Model ID ^a	M_{mc} ^b	$SFR - m_{\max}$ ^c	$m_{\text{agb},1}$ ^d	C_{sf} ^e
M1	1.0	—	4.0	9.0
M2	1.0	A	4.0	9.0
M3	1.0	A	3.0	9.0
M4	1.0	A	3.0	18.0
M5	1.0	B	3.0	9.0
M6	0.1	A	3.0	9.0
M7	0.3	A	3.0	9.0
M8	3.0	A	3.0	9.0
M9	1.0	— (fixed m_{\max})	3.0	9.0
M10	1.0	A (top-heavy IMF)	3.0	9.0
M11	1.0	A	3.0	4.5

^a M1 is the model in which truncation of star formation by SNe is not considered at all. A canonical (fixed) IMF is adopted in M9, m_{\max} is also a constant ($100M_{\odot}$; fixed duration of star formation in later generations of stars) The IGIMF theory is adopted for M2-M9 and M11 to calculate m_{\max} self-consistently. The IMF slope in the formation of 1G stars is assumed to be $\alpha = 1.35$ (top-heavy) for the model M10. The total mass of 1G in the GC of M11 is less than $10^6 M_{\odot}$ (less than 10% of the original gas mass).

^b The initial total mass of a GC-forming molecular cloud (MC) in units of $10^7 M_{\odot}$

^c ‘A’ and ‘B’ represent the model name for the physical relation between SFR (star formation rate) and m_{\max} (the maximum mass of stars in the adopted variable IMF). The details of models A and B are given in the main text and Fig. 1.

^d The lower mass cut-off (M_{\odot}) of AGB stars above which AGB ejecta is assumed to be converted into new stars.

^e Star formation coefficient. See eq. (2).

2.1 Basic equations in one-zone models

We adopt “one-zone” models of GC formation (i.e., 1G and LG formation) in which a GC is assumed to form through a continuous gas infall onto the core of a GC-forming MC with the initial total mass of M_{mc} . The basic equation for the evolution of gas and new stars is as follows:

$$\frac{dM_g}{dt} = -\psi(t) + A(t) + w(t), \quad (1)$$

where M_g is the total gas mass within the star-forming core of the MC, $\psi(t)$ is the star formation rate, $A(t)$ is the rate of gas accretion onto the core of the MC, and $w(t)$ is the injection rate of gas from its AGB stars. The star formation rate $\psi(t)$ (SFR) is assumed to be proportional to the gas mass (M_g) with a constant star formation coefficient and thus is described as follows:

$$\psi(t) = C_{\text{sf}} M_g(t). \quad (2)$$

This parameter C_{sf} describes the rapidity of star formation within a GC-forming MC. Since the present one-zone model can not investigate the details of star formation processes within GC-forming MCs, we need to adopt a reasonable value for C_{sf} . Our recent hydrodynamical simulations of star formation in GC-forming MCs with $M_{\text{mc}} = 10^7 M_{\odot}$ shows that (i) the peak star formation for 1G stars is about $1M_{\odot} \text{ yr}^{-1}$ and (ii) the peak star formation in LG stars is $[0.001-0.01]M_{\odot} \text{ yr}^{-1}$ (see Fig. 6 in B17b). These are broadly consistent with the results of the fiducial model with $C_{\text{sf}} = 9$, which means that the adopted C_{sf} is reasonable and realistic. Furthermore, the models with the adopted $C_{\text{sf}} = [9-18]$ demonstrate that the total mass of 1G stars can be larger

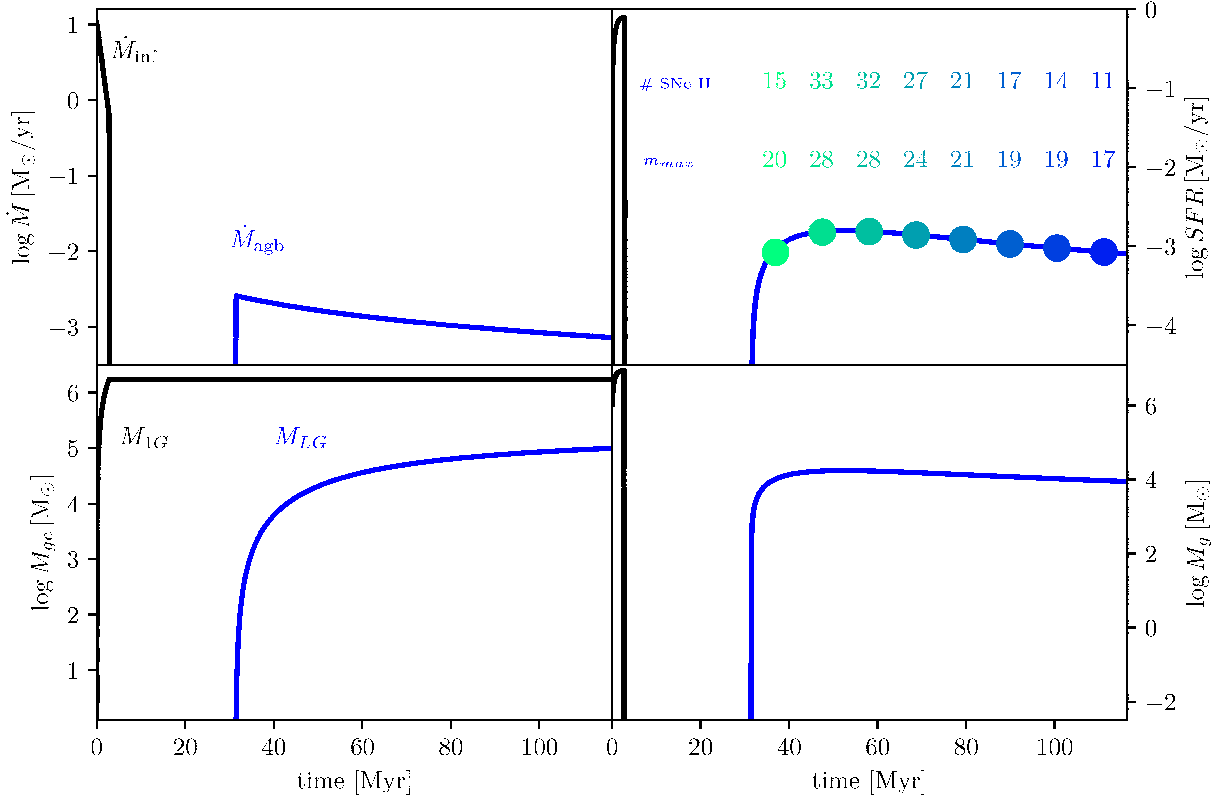


Figure 2. Time evolution of gas accretion and AGB ejection rates (upper left), SFR (upper right), total masses of stars in 1G and LG (lower left), and total gas mass (lower right) in the model M1 (See the details of the model parameter in Table 2). The total number of type II SNe (N_{SNII}) and m_{\max} in units of M_{\odot} (maximum mass of stars) in each of the selected time intervals are shown in the upper right panel. The end of 1G star formation at $T \approx 30$ Myr corresponds to $T = 0$ in Fig.3.

than $\approx 10^6 M_{\odot}$ for $M_{\text{mc}} \approx 10^7 M_{\odot}$. This means that an enough amount of gas can be ejected from AGB stars for LG formation. Since a large fraction of 1G stars can be lost in the later evolution of a GC (e.g., Vesperini et al. 2011; Rossi et al 2016), the initial mass of FG stars should be as large as $\approx 10^6 M_{\odot}$ for a typical GCs with the present-day mass of $M_{\text{gc}} = 2 \times 10^5 M_{\odot}$ to be formed.

We assume that C_{sf} is the same for 1G and LG formation in the present study. The present models with a constant C_{sf} is quite reasonable, because they can predict star formation histories of 1G and LG that are similar to those derived by fully self-consistent hydrodynamical simulations of GC formation (Bekki 2017b). Also, it is not realistic for the present study to adopt a variable C_{sf} , because it is theoretically unclear how C_{sf} depends on physical properties of GC-forming MCs.

Conroy & Spergel (2011) suggested that the effects of Lyman-Werner (LW) photons from 1G stars on H_2 (in AGB ejecta) are very important, because they can prevent secondary star formation owing to the dissociation of H_2 . However, they did not consider the importance of H_2 self-shielding from the intense LW radiation. Such a self-shielding effect is very important for gas with H_2 column density (N_{H_2}) significantly larger than 10^{14} cm^{-2} (e.g., Draine & Bertoldi 1996). The reduction factor (f_{red}) can be approximated described as follows:

$$f_{\text{red}} = \left(\frac{N_{\text{H}_2}}{10^{14} \text{ cm}^{-2}} \right)^{-0.75}. \quad (3)$$

A lower f_{red} means that a larger amount of LW photons can be self-shielded by H_2 (See Draine & Bertoldi 1996 for a more complex functional form for f_{red}). As shown in our recent simulations (B17b; Bekki & Tsujimoto 2017), the density of intra-cluster gas ejected from AGB stars (Σ_{icm}) in a forming GC can be much higher than 10^{14} cm^{-2} ($\Sigma_{\text{H}_2} > 10^{22} \text{ cm}^{-2}$) within the central 1pc. This means that the suggested suppression of star formation by the LW photons is completely negligible. Thus, our assumption of LG formation soon after gas accumulation in the centers of GCs is reasonable.

We consider that the formation of 1G stars can be truncated by SNe 3×10^6 yr after the initial burst of star formation in a GC-forming MC. This SF-duration (Δt_{sf}) corresponds to the lifetime of the most massive star (with a mass of $\approx 100 M_{\odot}$) within the MC. We also consider two different models for star formation from AGB ejecta of 1G stars in a GC as follows. One is that star formation can continue over ≈ 400 Myr without any interruption of star formation by energetic events such as supernova (SNe). (‘continuous model’). The other is that star formation can be truncated by SNe from LG stars owing to the strong thermal and kinematic feedback (‘multiple burst model’, though, literally, it is not a burst but a sporadic low-level star formation). In the previous one-zone GC formation models (e.g., B07; D08, D10), star formation from AGB ejecta was assumed to be continuous for a certain timescale (of an order of 10^8 yr). However, we consider that such an assumption is highly unrealistic, given the lifetime of massive stars with $m > 10 M_{\odot}$.

is quite short (less than 2×10^7 yr). We here investigate mainly a number of multiple burst models, though we investigate the continuous models too just for comparison.

In the multiple burst model, C_{sf} is set to be 0 when the most massive star with a mass of m_{max} within a generation of stars (e.g., 2G, 3G, and 4G) explodes as a SN. All of the remaining gas (i.e., AGB ejecta) is assumed to be expelled owing to the strong SN feedback effects after the SN (i.e., $\text{SFR}=0$). Accordingly, the duration of star formation (Δt_{sf}) corresponds to the lifetime (t_{lf}) of the most massive star ($t_{\text{lf}}(m_{\text{max}})$). Both C_{sf} and M_{g} are set to be 0 until all of the SNe are exploded, and this period of SF truncation is denoted as Δt_{tr} . We adopt a fixed Δt_{tr} of 3.2×10^7 yr for all models in the present study, since it approximately corresponds to the $[8-9]M_{\odot}$ SN. Recent studies of the IMF have demonstrated that the IMF can be time-evolving and depend on a few key parameters of star-forming regions, such as metallicity, SFR, and gas density (e.g., Marks et al. 2012; Kroupa et al. 2013). In order to estimate m_{max} in each episode of star formation, we use the results of these theoretical studies on the correlation between SFR and m_{max} (e.g., Kroupa et al. 2013; Yan et al. 2017; Stephens et al. 2017).

We adopt a standard $m - t_{\text{lf}}$ relation for stars with $m \geq 9M_{\odot}$ in order to derive the $\text{SFR} - \Delta t_{\text{sf}}$ relation from the $\text{SFR} - m_{\text{max}}$ relation. Fig. 1 shows the adopted two models for the $\text{SFR} - \Delta t_{\text{sf}}$ relations. Model A is consistent with the theoretically derived one by Yan et al. (2017) whereas m_{max} in model B is by a factor of 2 smaller than that in model A. Therefore, Δt_{sf} is appreciably longer in model B than in model A. This model B could be also derived from the IGIMF theory for star clusters, if the mass function of very young clusters becomes bottom heavy at low SFRs. We estimate Δt_{sf} at each time step, $T = t_i$, using the $\text{SFR} - \Delta t_{\text{sf}}$ relation and compare Δt_{sf} with $t_i - t_{\text{start}}$, where t_{start} is the time at which star formation started. If Δt_{sf} is shorter than $t_i - t_{\text{start}}$, then star formation is truncated from $T = t_i$ to $T = t_i + \Delta t_{\text{tr}}$.

For the accretion rate, we adopt $A(t) = C_{\text{a}} \exp(-t/t_{\text{a}})$ and t_{a} is set to be 10^6 yr. We confirm that the present results do not depend on t_{a} as long as it is shorter than 3×10^6 yr. The normalization factor C_{a} is determined such that the total gas mass accreted from AGB ejecta onto the core of a MC can be M_{mc} for a given t_{a} . In order to estimate the total mass of AGB ejecta in a GC, we adopt the IMF that is defined as $\Psi(m) = C_0 m^{-\alpha}$, where m is the initial mass of each individual star and the slope $\alpha = 2.35$ corresponds to the canonical IMF (Salpeter 1955; Kroupa 2001). The normalization factor C_0 is a function of α , m_{l} (lower mass cut-off; $0.1M_{\odot}$), and m_{u} (upper mass cut-off). We investigate models with different α to discuss how the total mass of ejecta from AGB stars depend on α and how it can influence the SFR of LG stars. It should be noted here that although this single power-law IMF for 1G is not so realistic as those adopted in recent IMF studies (e.g., Marks et al. 2012; Kroupa et al. 2013), this approximation is sufficient for the purpose of predicting the total mass of AGB ejecta in this study.

The total mass of gas ejected from AGB stars between $T = t$ and $T = t + \delta t$ (M_{agb}), where δt is the time step width, is described as:

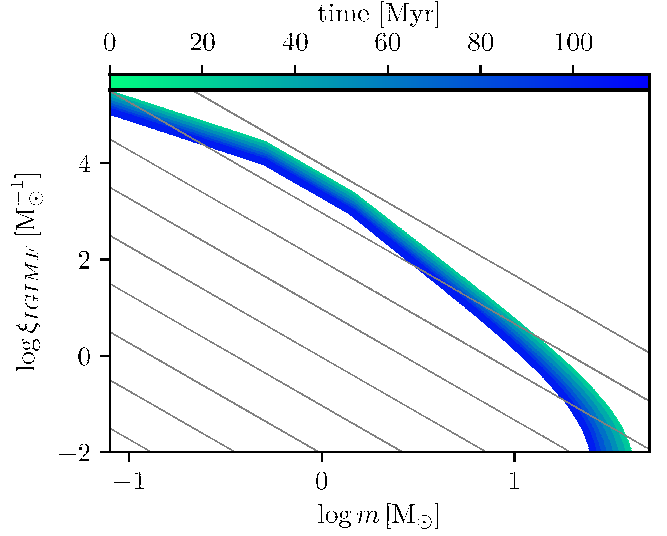


Figure 3. IGIMF as a function of stellar mass (m) at different epochs in the model M1. At early times, the IGIMF is less top-light whereas it is less top-heavy at later times (when SFR decreases with time). The diagonal lines indicate the canonical IMF with $\alpha = 2.35$.

$$M_{\text{agb}} = \int_{m_{\text{agb}}(t+\delta t)}^{m_{\text{agb}}(t)} m_{\text{ej}} \Psi(m_{\text{ini}}) dm_{\text{ini}}, \quad (4)$$

where m_{ej} describes the total gas mass ejected from an AGB star with initial mass m_{ini} and final mass (m_{fin}). The lowest ($m_{\text{agb}}(t + \delta t)$) and highest masses ($m_{\text{agb}}(t)$) of AGB stars at $T = t$ correspond to the masses of stars which enter into the main-sequence turn-off at $T = t + \delta t$ and $T = t$, respectively. We adopt the following analytic form of m_{ej} derived by Bekki (2011) based on observational results by (Weidemann 2000):

$$m_{\text{ej}} = 0.916 m_{\text{ini}} - 0.444, \quad (5)$$

where m_{ej} and m_{ini} are given in units of M_{\odot} . Thus, the AGB wind rate is as follows:

$$w(t) = \frac{dM_{\text{agb}}}{dt} \quad (6)$$

In order to calculate t_{lf} of stars with $m \leq 9M_{\odot}$, we use the mass-age relation by Renzini & Buzzoni (1986; 2010).

2.2 IGIMF

The standardly made assumption is that the 1G and LGs are formed with an invariant IMF. This leads to the problem that the LGs produce too many SN explosions which inhibit the build-up of the LGs such that the AGB scenario for LGs has been often thought to be less realistic. Closer scrutiny of the observational data however indicates that star formation occurring in embedded clusters might result in a non-standard IMF (i.e., non-standard composite IMF of the whole stellar populations in all clusters). Even previously-thought distributed star formation has been found to be organized in embedded clusters (e.g. fig.12 in Megeath et al. 2016), whereby low-intensity star formation produces low-mass embedded clusters (ECs) only. Low-mass ECs do not contain massive stars because the molecular gas mass is distributed over the stellar population in the form of a largely

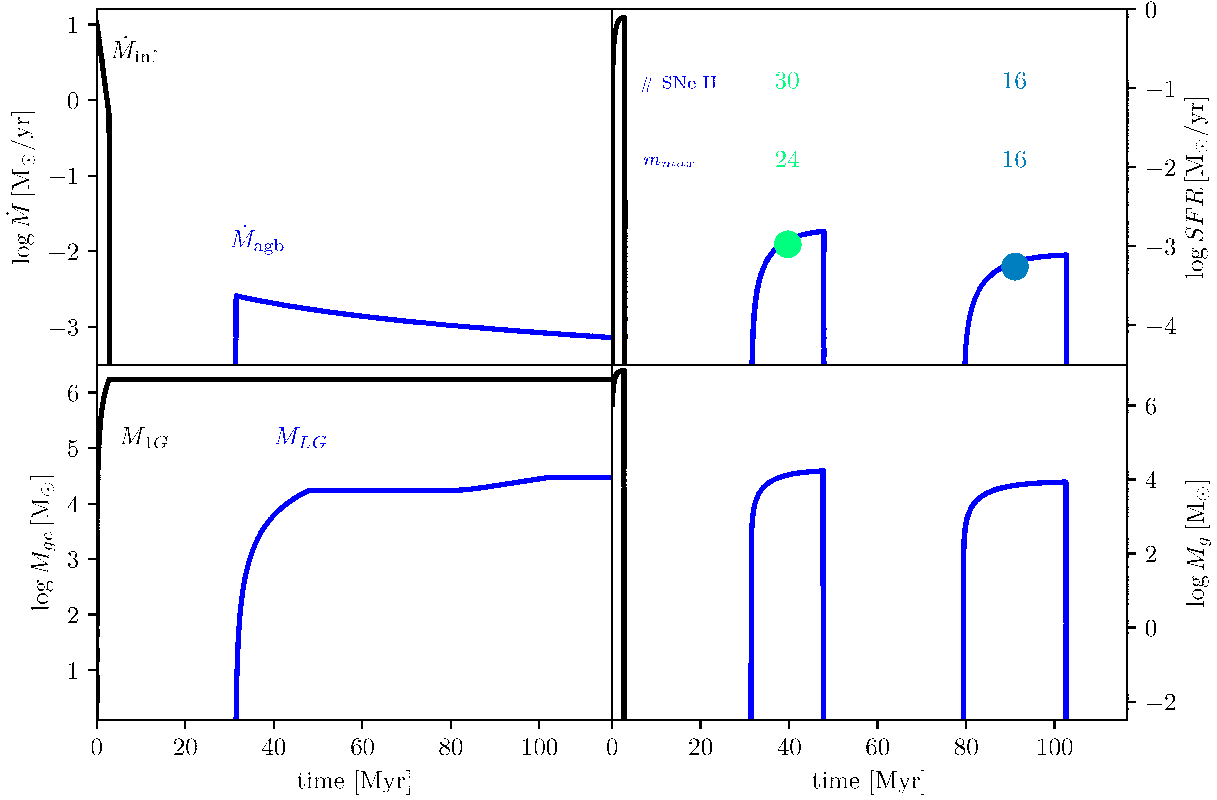


Figure 4. The same as Fig. 2 but for M2 in which the duration of star formation is self-consistently derived from the evolution of the SFR.

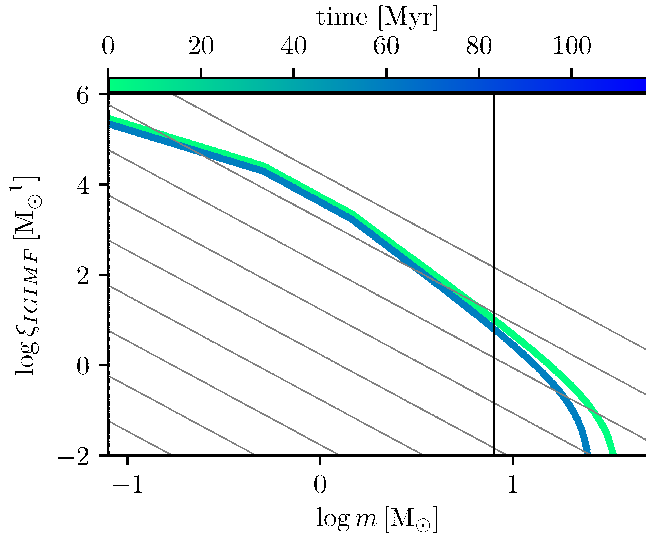


Figure 5. The same as Fig. 3 but for M2.

invariant IMF (Kroupa 2002; Bastian et al. 2010; Marks et al. 2012; Kroupa et al. 2013) leaving not enough mass to form a massive star within the EC. Thus, for example, there is a significant deficit of massive stars in the low-density Orion A cloud (Hsu et al. 2013). Indeed, the existence of a correlation between the most-massive-star (m_{\max}) and the stellar mass in the embedded cluster (M_{ec1}) has been found to be highly significant (Weidner et al. 2013, 2014; Stephens et al. 2017; Ramirez Alegria et al. 2016).

The mathematical formalism of the IGIMF theory (e.g. Recchi & Kroupa 2015; Fontanot et al. 2017; Yan et al. 2017) can be applied to the problem at hand, namely the formation of the LG from AGB ejecta in young GCs. The key relation which is of relevance for this problem is the $m_{\max} - \text{SFR}$ relation and as well that the IMF of the LG (i.e. the IGIMF) has a non-canonical shape above about $1 M_{\odot}$ by being top-light for the relevant physical situation here given by the small SFRs of the LGs. The combination of these two implications lead to a significantly smaller number of SN events produced by the LGs such that star-formation from AGB ejecta can, contrary to the case of an invariant canonical IMF, build-up to a very significant mass with the added conclusion that this LG star formation must be truncated semi-periodically by the few SN events that do occur in the LG when the SFR is sufficiently high. This is shown by simulations in the following sections.

2.3 Chemical yields of AGB ejecta

The present one-zone model is quite different from B17 in that it does not include chemical evolution explicitly. Accordingly, the model can not predict the chemical abundances of GC stars in a fully self-consistent way. However, we investigate the possible internal spreads in chemical abundances of light elements among GC stars by allocating the abundances for each star formation episode in GC formation. We particularly investigate the $[\text{Mg}/\text{Fe}]$ and $[\text{Al}/\text{Fe}]$ abundances of GC stars by using the chemical yields table derived by Ventura et al. (2009, 2011). Since the tables by

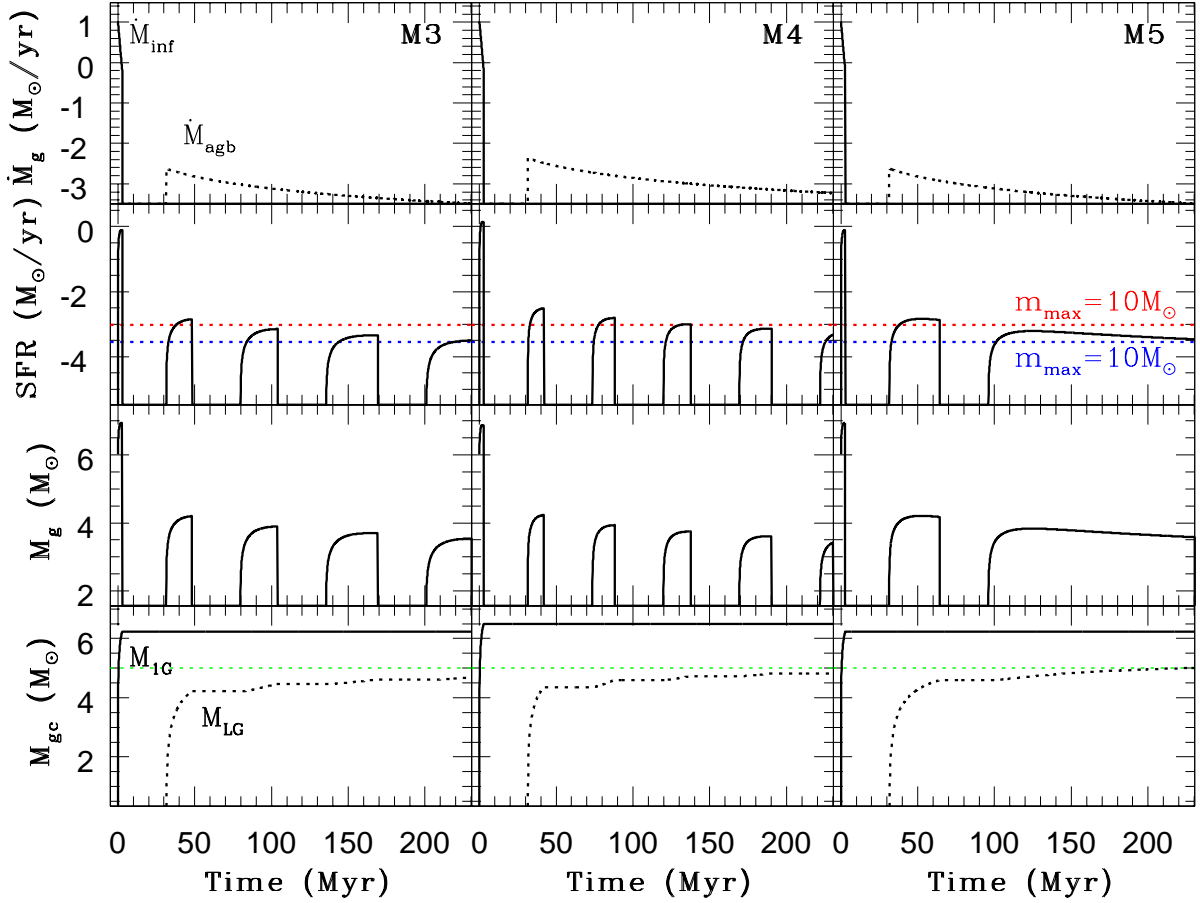


Figure 6. Time evolution of gas accretion rate and AGB ejection rate (top), SFR (second from the top), total gas mass (second from the bottom) total masses of stars in 1G and LG (bottom), for M3 (left), M4 (middle), and M5 (right). The blue (upper) and red (lower) horizontal lines (in the SFR evolution) represent the SFRs corresponding to $m_{\text{max}} = 10M_{\odot}$ in model A and B, respectively. The green line in the bottom panel indicates the typical mass of 2G stars observed in the Galactic GCs (C09).

Ventura et al. (2009, 2011) are only for 12 different masses of stars (i.e., 12 metallicity bins), we use an interpolation method to calculate $[\text{Mg}/\text{Fe}]$ and $[\text{Al}/\text{Fe}]$, if a star has an abundance between two metallicity bins.

We investigate the $[\text{Mg}/\text{Fe}]-[\text{Al}/\text{Fe}]$ anti-correlation which is already known to be produced by the AGB scenario reasonably well (e.g., B07, D10, Ventura et al. 2016). The currently available chemical yields tables from Karakas (2010) and Ventura et al. (2011), however, cannot reproduce the Na-O anti-correlation so well. This possibly problematic feature of the AGB scenario in general is beyond the scope of this paper (we may focus more on this issue in forthcoming papers).

2.4 Parameter study

Although we have investigated many models with different model parameters (e.g., C_{sf} , t_a , α , Δt_{sf} , M_{mc} etc), we here describe the results of 11 representative models. The parameter values for these models are given in Table 2. The model M1 is the continuous model in which the SF histories of GCs is not influenced at all by SNe (which is highly unrealistic). Other models, M2-M10, are the multiple burst models, which can show multiple generations of stars in form-

ing GCs. Since the purpose of this paper is to understand the origin of discrete multiple stellar populations of GCs, we almost exclusively describe the results on these multiple burst models in the present study. The results of the multiple burst models with a canonical IMF for all stellar populations (M9) and a top-heavy one for 1G stars (M10) are given in Appendix A, because their results are not as important compared with the other models. Also the results of M11 are not discussed here, because the final mass of 1G stars is less than 10% of the original gas mass, which means that the initial cluster can be completely disintegrated after gas removal owing to the low star formation efficiency (e.g., Hills 1980): see Appendix B for the results. The details of the IGIMF theory are also summarized in Appendix C.

3 RESULTS

3.1 Star formation histories of forming GCs

Fig. 2 shows that 1G stars with $M_{1G} = 1.7 \times 10^6 M_{\odot}$ can be formed from a molecular cloud with $M_{\text{mc}} = 10^7 M_{\odot}$ within a timescale of ≈ 3 Myr in the continuous model M1. The star formation rate for 1G population is as high as $[0.1-1]M_{\odot}$

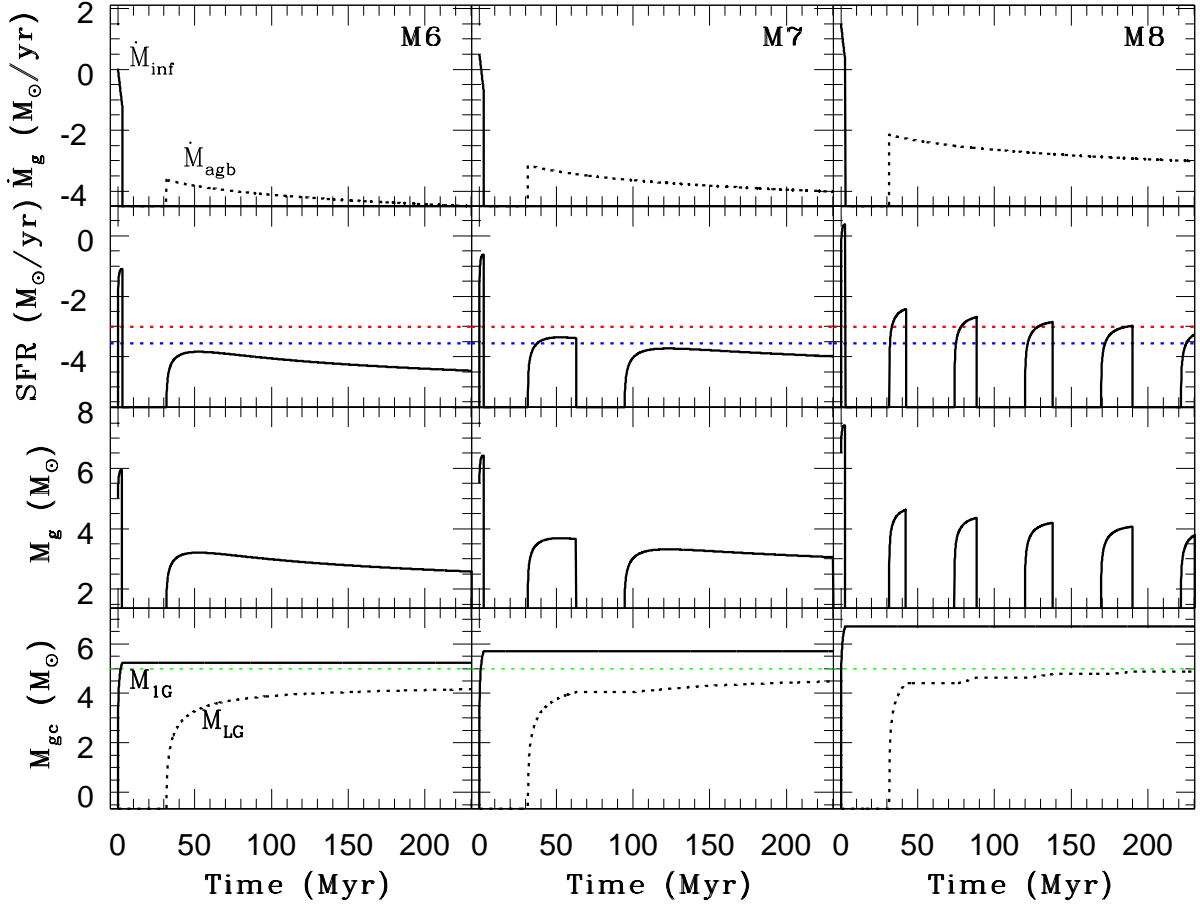


Figure 7. The same as Fig. 6 but for M6 (left), M7 (middle), and M8 (right).

yr^{-1} owing to the initial high gas density of the MC. The star formation of 1G stars is truncated by the most massive SNe with $m > 100M_{\odot}$ in the model with a canonical IMF. All of the remaining gas within the MC ($8.3 \times 10^6 M_{\odot}$) is expelled from the MC by the SNe so that the gas can not be converted into new stars after $T = 3.2$ Myr (i.e., star formation efficiency, $\epsilon_{\text{sf}} = M_{1\text{G}}/M_{\text{mc}} = 0.17$). About 30 Myr after the initial burst of star formation, massive AGB stars with $m = 9M_{\odot}$ start to inject the gas into the 1G stellar system. The gas is then slowly converted into 2G stars with a very low SFR ($< 10^{-2} M_{\odot} \text{ yr}^{-1}$) and this secondary star formation can continue until intermediate-mass stars with $m = 4M_{\odot}$ enter into their AGB phases ($T = 120$ Myr). The total mass of the 2G stars can finally become $M_{2\text{G}} \approx 10^5 M_{\odot}$, being consistent with the observed typical mass of 2G stars for the Galactic old GCs (C09).

Fig. 3 shows that if we adopt the IGIMF model which depends on the SFR, then the IMF of the GC in M1 can evolve significantly even within 120 Myr. The number of SNe II (N_{SNII}) predicted from the IGIMF (181) is much smaller than that from the canonical IMF (≈ 1100) for the 2G stars (Also see Fig. 2 for the evolution of N_{SNII}). Furthermore, m_{max} is smaller in the later phase of 2G formation (e.g., $24M_{\odot}$ at $T = 40$ Myr and $17M_{\odot}$ at $T = 110$ Myr) and the mean m_{max} is smaller in the IGIMF ($24M_{\odot}$) than in the canonical IMF ($= 120M_{\odot}$). These results are due to the

very low SFR of 2G formation for which the IGIMF theory predicts lower m_{max} . However, given the SFR, the derived m_{max} from the IGIMF can not be smaller than $10M_{\odot}$ in this model, which means that SNe should be able to severely suppress or even truncate the 2G formation. Therefore, the continuous formation of 2G stars over 100 Myr is inconsistent with m_{max} and a large number of SNe in the continuous model with a canonical IMF. We thus suggest that previous models of GC formation based on self-enrichment by AGB stars are not so realistic.

Fig. 4 shows the results of M2 in which the SF duration of LG stars is self-consistently derived from the adopted $\text{SFR} - \Delta t_{\text{sf}}$ relation. Although star formation in the 2G formation can be truncated by SNe in this model, the SF duration can be as long as 16 Myr owing to the low-mass of the most massive SN with $m = m_{\text{max}} = 24M_{\odot}$. It should be stressed here that if the canonical IMF is adopted indeed, then the SF duration is only $\approx 3 \times 10^6$ yr owing to $m_{\text{max}} \approx 120M_{\odot}$. After the explosion of the lowest-mass SN ($m = 9M_{\odot}$), 3G stars are formed from AGB ejecta with a lower SFR. The duration of 3G formation can be longer than that of 2G owing to the lower SFR of 3G formation (i.e., lower m_{max}).

Fig. 5 demonstrates that not only the shape of the IMF but also m_{max} can be different between 2G and 3G stars, if the IGIMF theory is adopted as a basis of the calculation.

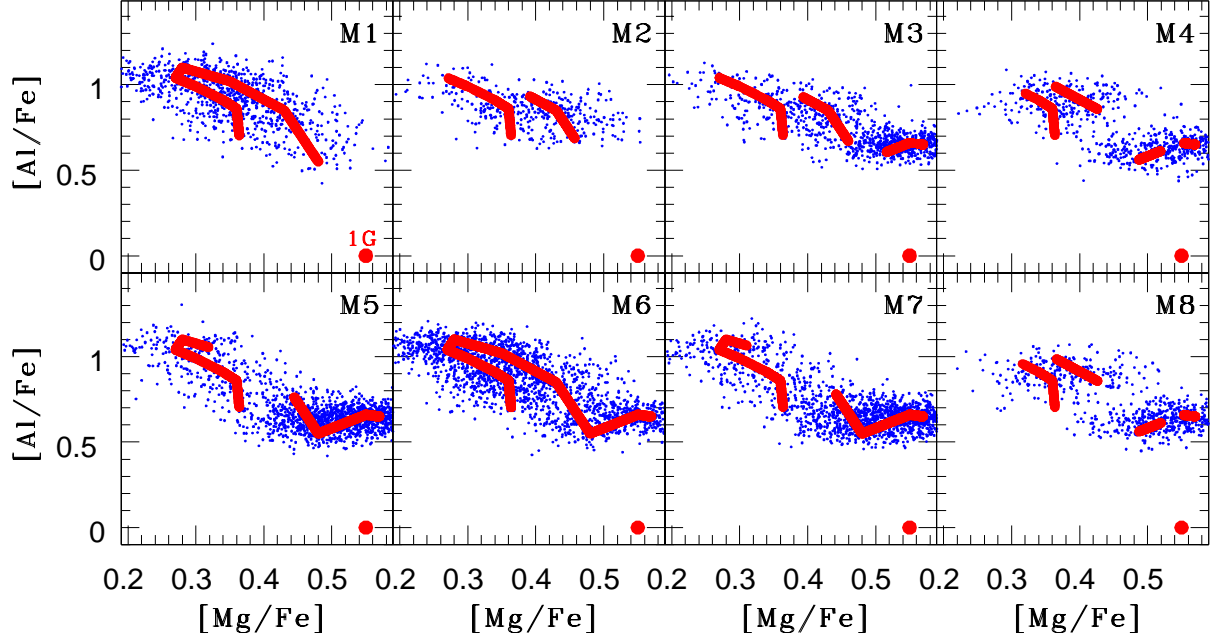


Figure 8. Distributions of LG stars (big red dots) on the $[\text{Mg}/\text{Fe}]$ - $[\text{Al}/\text{Fe}]$ diagram for the eight models (M1-M8). The small blue dots show the distribution of GC stars created by adding random observational errors of 0.05 dex to the original simulation data sets. Each model ID is indicated in the upper right corner of each frame. For comparison, the location of 1G stars is indicated by one big red dot with characters “1G” above it.

This model can not have $m_{\text{max}} < 10M_{\odot}$ in 2G and 3G formation, if the standard model A for the $SFR - \Delta t_{\text{sf}}$ relation is adopted. The large number of SNe ($N_{\text{SNI}} = 131$) means that the remaining AGB ejecta can be blown away by SNe, which is consistent with the truncation of SF by SNe in this model M2. The final mass of LG stars in this model, however, is $3.0 \times 10^4 M_{\odot}$, which is significantly lower than that of M1. This suggests that M_{mc} or $m_{\text{agb},1}$ should be larger and lower, respectively, for such multiple burst model to have $M_{\text{LG}} \approx 10^5 M_{\odot}$.

Fig. 6 shows the three multiple burst models with $m_{\text{agb},1} = 3M_{\odot}$ yet different C_{sf} and $SFR - \Delta t_{\text{sf}}$ relations. The GC in M3 can finally have 1G, 2G, 3G, and 4G with $M_{\text{LG}} = 4.8 \times 10^4 M_{\odot}$ at $T = 230$ Myr. M4 with larger C_{sf} (thus larger $M_{1\text{G}}$) shows 5 distinct generations of stars with a higher SF and shorter SF duration due to the higher SFR in each SF episode. The final M_{LG} can be therefore larger ($6.8 \times 10^4 M_{\odot}$) than that of M2. M6 with the model B $SFR - \Delta t_{\text{sf}}$ relation shows only two LG populations with the 3G still forming at $T = 230$ Myr. The very long SF duration in the 3G results from the lower m_{max} . This lower m_{max} is due to the adopted $SFR - \Delta t_{\text{sf}}$ relation (model B) in this model. The GC in this model can finally have $M_{\text{LG}} = 1.0 \times 10^5 M_{\odot}$ as M1, which is more consistent with observations (C09). Although there is little scatter in the observed $SFR - m_{\text{max}}$ relation (thus $SFR - \Delta t_{\text{sf}}$ relation) for star-forming regions of the Galaxy (Weidner et al. 2013), the relation can be different in the central region of forming GCs, as mentioned above. Thus, the results of M5 with a non-standard $SFR - \Delta t_{\text{sf}}$ relation are quite interesting in the sense that M_{LG} is more consistent with the observed typical value for the Galactic GCs than M2 with the standard relation.

Fig. 7 describes how the SFRs of forming GCs depend on their parent MC masses. The low-mass MC model M6 with $M_{\text{mc}} = 10^6 M_{\odot}$ shows no truncation of star formation in LG, because m_{max} becomes less than $9M_{\odot}$ owing to very low SF during 2G formation. This result implies that low-mass GCs are unlikely to have discrete multiple stellar populations. Although the less-massive model M7 with $M_{\text{mc}} = 3 \times 10^6 M_{\odot}$ shows 2G and 3G formation, m_{max} becomes less than $9M_{\odot}$ in the 3G formation so that 3G star formation can not be truncated. Interestingly, the mass-ratios of LG to 1G in these models are higher than those derived for M3 with $M_{\text{mc}} = 10^7 M_{\odot}$, because the formation of LG stars can continue longer in these models.

Fig. 7 also shows that the SFR during the formation of LG stars is significantly higher in the massive GC model M8 with $M_{\text{mc}} = 3 \times 10^7 M_{\odot}$. As a result of this, the duration of the star formation is shorter owing to higher m_{max} ($\approx 60M_{\odot}$). Therefore, the GC in M8 can finally have 5 distinct stellar populations at $T = 230$ Myr: one more stellar population in comparison with M2. The shorter duration of star formation in 1G and 2G implies that the abundance spread in these generations can be small. The final mass of LG stars (M_{LG}) becomes as large as $10^5 M_{\odot}$, which is consistent with the observed typical M_{LG} of the Galactic GC. These results of the three models suggest that the numbers of discrete stellar populations in GCs depend on the initial masses of GCs.

4 DISCUSSION

4.1 Internal abundance spreads in discrete stellar populations

The multiple generations of stars formed in several GC formation models of the present study (e.g., M2 and M3) strongly suggest that discrete stellar populations can be seen in the [Na/Fe]-[O/Fe] and [Mg/Fe]-[Al/Fe] diagrams of GC stars. It is thus our important investigation whether such discrete populations can be really seen in the [Mg/Fe]-[Al/Fe] diagram. The purpose of this investigation is not to reproduce the observed [Mg/Fe]-[Al/Fe] anti-correlations (e.g., Ventura et al. 2016) but to illustrate whether distinct groups of stars in the [Mg/Fe]-[Al/Fe] diagram can be clearly seen in the present models. More detailed investigation of each individual objects (such as M13) will need to be done in our future studies with more sophisticated modeling of GC formation. As shown in Fig. 8, the GC at the final time step in M1 has two distinct groups of stars on the [Mg/Fe]-[Al/Fe] diagram, and the two groups are well separated from the location of 1G stars. The GC in M1, on the other hand, has a continuous distribution of stars along the expected [Mg/Fe]-[Al/Fe] anti-correlations. The GCs in the models M3 and M4 with longer duration of LG star formation has four and five discrete stellar populations, respectively, though the locations of 3G, 4G, and 5G on the diagram are hard to be distinguished in M3. A wide gap between the locations of 2G and 3G stars can be seen in the GC of M3 with a long duration of 3G star formation.

As expected from star formation histories of GCs in M6-M8, only more massive GCs formed from $M_{\text{mc}} \geq 3 \times 10^6 M_{\odot}$ can have discrete stellar populations on the [Mg/Fe]-[Al/Fe] diagram. The distribution of each sub-population appears to be narrower in M8, which reflects the fact that the duration of LG star formation episodes are shorter in this model. This suggests that discrete stellar populations on the [Mg/Fe]-[Al/Fe] diagram can be more clearly seen in more massive GCs. Although this ‘mass-dependent visibility of discreteness’ is an important prediction of the present model of GC formation based on the IGIMF, it is at present not observationally clear whether such discreteness can be more clearly seen in more massive GCs owing to the small number of GCs investigated with more precise abundance measurements (e.g., C14).

Errors in observational measurements of [Mg/Fe] and [Al/Fe] can broaden the narrow distribution of stars along the original tight Mg-Al anti-correlation so that the discrete stellar populations may appear much less pronounced. Observational errors in the abundance estimation ([A/Fe], where A is a light element) ranges typically from 0.031 to 0.076 in C09, which is not negligible in comparison with the possible differences of [A/Fe] between LG stars predicted from the present study. It is therefore possible that the observed apparent continuous distributions of GC stars along the Mg-Al anti-correlation is indeed due to the broadening through observational uncertainty of the original discrete stellar populations (C14). In order to investigate this issue, we created new distributions of GC stars on the [Mg/Fe]-[Al/Fe] diagram in each model by adding random errors to the original simulation data. Dispersions of 0.03, 0.05, and 0.1 dex are added to [Mg/Fe] and [Al/Fe] in the original simulation data in order for us to investigate whether orig-

inal discrete distributions of GC stars can disappear owing to the addition of such small observational errors.

Small dots in Fig. 8 show the the new distributions that are created by adding 0.05 dex random errors to the original simulation data. Clearly the distributions now appear much less discrete along the Mg-Al anti-correlation. It is furthermore confirmed that this almost disappearance of the discrete distributions can be seen in the new distributions with 0.03 and 0.1 dex random errors added to the original data. These results therefore suggest that the observed apparently continuous distributions of GC stars along the Mg-Al anti-correlation (and Na-O one) do not necessarily mean that the true distribution is continuous too. They also suggest that more precise estimation of Mg and Al abundances is necessary for many GCs to discuss whether GCs experienced multiple episodes of star formation separated by of the order of 10^7 yr.

The key physical processes for the formation of discrete multiple populations are the following three. First is the truncation of star formation from AGB ejecta by SNe in each generation of stars. Second is the relatively long interval (≈ 20 Myr) between the formation of two generations of stars. Third is the time-evolving IMF during GC formation, which ensures the longer duration (> 10 Myr) of star formation in each generation. Although the ‘top-light’ IMF is required to lengthen the duration of star formation, an overly top-light IMF without SNe can not explain the presence of discrete stellar populations in GCs, because it allows AGB ejecta to continue to be converted into new stars. As demonstrated in Appendix A, the model with a canonical universal IMF (M9) predicts very small total masses of later generations of stars ($M_{\text{LG}} = 0.0002 M_{\text{mc}}$), which means that typical GCs would need to be formed from super-giant MCs with $M_{\text{mc}} \approx 5 \times 10^8 M_{\odot}$. But this required M_{mc} appears to be too large to be realistic: GC formation models with a time-evolving IMF appears to be more realistic.

The present study predicts that more massive GCs are more likely to have at least a few discrete multiple stellar populations. Such massive GCs can possibly have six discrete populations, if new stars can continue to be formed from ejecta of AGB stars until stars with $m = 3M_{\odot}$ become AGB stars. (i.e., until ≈ 400 Myr after the initial starbursts). So far NGC 6752, M22, and NGC 2808 have been observed to show three or more discrete stellar populations in the [Na/Fe]-[O/Fe] and [Mg/Fe]-[Al/Fe] relations and the color-magnitude diagrams (C14; Marino et al. 2011) and these are massive GCs. Currently it is not observationally clear whether GCs with lower masses (yet with multiple stellar populations) have discrete stellar populations or not. Apparently, all of the GCs with multiple stellar populations in C09 appear to show continuous populations in the [Na/Fe]-[O/Fe] diagrams. However, these apparently continuous stellar populations could be due largely to observational errors in the estimation of chemical abundances by previous spectroscopic observations. It is thus doubtlessly worth while for observational studies to investigate the distributions of stars on the [Na/Fe]-[O/Fe] and [Mg/Fe]-[Al/Fe] diagrams of many GCs to gain a better understanding of the origin of the discrete multiple stellar populations.

4.2 Lack of OB stars in LG star formation – the case of young massive clusters (YMCs)

Recent observational studies have searched for evidence of ongoing star formation in young massive clusters (YMCs) in nearby galaxies and found no evidence for it (e.g., Larsen et al. 2011; Bastian et al. 2013; Cabrera-Ziri et al. 2014). For example, Bastian et al. (2013) investigated $H\beta$ and $[OIII]$ emission lines of 130 YMCs with ages ranging from 10 Myr to 1000 Myr and found no evidence of such emission lines in the YMCs. Since stellar radiation from massive OB stars are responsible for such emission lines, they concluded that secondary star formation lasting over hundreds of Myr can be ruled out by their observations. Cabrera-Ziri et al. (2014) investigated the stellar population of a YMC with a mass of $\approx 10^7 M_\odot$ and found that its spectral energy distribution (SED) is consistent with a single stellar population with an age of ≈ 100 Myr. Goudfrooij et al. (2014), however, criticized these interpretations of YMCs and pointed out that the observations can not rule out the secondary star formation in the YMCs.

The present study has shown that m_{\max} (the maximum mass of stars) can be well less than $30 M_\odot$ during secondary star formation in star clusters. Therefore, the observed apparent lack of massive OB stars in YMCs of nearby galaxies can result not from the absence of secondary star formation within the YMCs but from a lower m_{\max} in secondary star formation within the YMCs. Accordingly, the lack of $H\alpha$ emission lines in YMCs can not rule out secondary star formation: other diagnostic observations are required to distinguish between the above two scenarios for the lack of $H\alpha$ emissions in clusters. If LG stars are formed with a top-light IMF (i.e., low m_{\max}) in a forming GC, as demonstrated in the present study, then the SED of the GC would not be influenced by the less dominant LG stars when the GC is ≈ 100 Myr old. That star formation can proceed without the formation of massive stars has been documented already in several observational papers (e.g., Kirk & Myers 2011; Hsu et al. 2013).

Indeed, For & Bekki (2017) have recently discovered young stellar objects (YSOs) within older star clusters with ages ranging from 0.1 Gyr to 1 Gyr in the LMC using the observational data obtained by Spitzer and Herschel. This discovery has clearly demonstrated ongoing (secondary) star formation is possible in the older star clusters of the LMC and would be possible in other YMCs of other galaxies. This discovery by large infrared telescopes suggests that secondary star formation can be more easily detected in infrared observations than in optical photometric and spectroscopic ones. It is currently a formidable task for observational studies to find dust-shrouded intermediate-mass and low mass stars with ages less than 1 Myr in YMCs of nearby galaxies. We suggest, however, that future observational studies on the presence or absence of YSOs in YMCs are indispensable for proving if secondary star formation in older YMCs can be ongoing.

4.3 Dilution of AGB ejecta with pristine gas

So far we did not discuss the importance of dilution of AGB ejecta with “pristine gas” (i.e., gas that has the same chemical abundances as 1G stars) in the formation of multiple

stellar populations of GCs. Previous one-zone chemical evolution models of GC formation already demonstrated that such dilution processes are essential for reproducing the observed Na-O, Mg-Al, and C-N anti-correlations and He abundance distributions (B07, D10). Accretion of gas onto the potential of a cluster from the surrounding ISM was expected from analytical calculations (Pflamm-Altenburg & Kroupa 2009). Recent hydrodynamical simulations of GC formation have demonstrated that gas accretion onto 1G stars of a GC from cold ISM surrounding the GC is possible in a GC-host dwarf galaxy (B17a). Such gas accretion has been demonstrated to occur ~ 50 Myr after the commencement of accretion of AGB ejecta onto the GC (Fig. 8 in B17a). This implies that new (LG) stars can be formed from pure AGB ejecta, if the new star formation occurs less than 50 Myr after gas ejection from the most massive AGB stars (M_\odot). A very small fraction ($\approx 1\%$) of cold gas within GC-forming MCs cannot be influenced by SNII and thus can be re-accreted onto 1G stellar systems (Fig. 1 in B17b). Such cold gas can be mixed with AGB ejecta to form LG stars (B17b). Gratton & Carretta (2010) proposed that gas from unevolved stars can be used for dilution of AGB ejecta.

Although the above-mentioned previous works clearly suggested the importance of dilution of AGB ejecta in GC formation, the time evolution of gas accretion onto existing GCs cannot be simply approximated by an analytic function. Therefore, we here discuss how the dilution process can possibly change the present results by assuming that AGB ejecta is mixed with the same amount of pristine gas: this assumption on the amount of pristine gas is quite reasonable (B07, D10). A factor of two increase in SFR is expected in this model with dilution owing to the adopted star-formation model. The adopted $\Delta t_{\text{sf}} - \log \text{SFR}$ relation for Model A (in Fig. 1) can be approximated by the following linear relation for $\log \text{SFR} \leq -3$ ($M_\odot \text{ yr}^{-1}$):

$$\Delta t_{\text{sf}} = -13.3 \times (\log \text{SFR} + 3.5) + 25.3. \quad (7)$$

This relation means that a factor of two increase in SFR from $\log \text{SFR} = -3$ to $\log \text{SFR} = -2.7$ (due to dilution) can shorten the duration of LG formation from 27.9 Myr to 21.8 Myr ($\sim 22\%$ decrease). This level of shortening is not so significant, and accordingly it would not change the present results (e.g., the total mass of LG stars etc) significantly. Therefore, we conclude that the roles of IGMF in the formation of discrete multiple populations do not depend strongly on whether dilution is included in the models or not.

Milone et al. (2017) have recently characterized the multiple stellar populations of 57 GCs using the photometric data from *Hubble Space Telescope* (HST) UV Legacy Survey of Galactic Globular Clusters. One of their remarkable results relevant to the present study is that some GCs show the split of both 1G and 2G populations (“Type II cluster” in their definition). They have shown that these Type II GCs with (at least) four populations are also enriched with iron and *s*-process elements. They have also found that some GCs have distinct stellar clumps along the 1G and 2G sequences whereas others have no such clumps. Although the presence (or absence) of such distinct groups of stars can be more robustly confirmed using a large number of stars (Milone et al. 2017), the origin of these GCs with distinct

multiple stellar populations can be explained by the scenario presented by this study.

The apparently smooth distributions along the 1G and 2G sequences observed in some GCs (Milone et al. 2017) cannot be simply explained by the present multiple-burst models. If such smooth distributions are observed only for low-mass GCs in Milone et al. (2017), they are consistent with the prediction of the present study (see Fig. 7). However, it is not clear whether GCs with such smooth distributions are more likely to be low-mass GCs in Milone et al. (2017). As shown in previous one-zone chemical evolution models with continuous star formation (B07 and D10), mixing (i.e., dilution) of AGB ejecta with pristine gas and the subsequent star formation would better explain the origin of such GCs. It is not well understood, however, how such dilution is possible in the early formation histories of GCs.

5 CONCLUSIONS

The present study has adopted a new GC formation model with a time-varying IMF (based on the IGIMF theory) in order to discuss the origin of discrete multiple stellar populations in GCs. The new model has incorporated the SFR - m_{\max} relation (e.g., Yan et al. 2017) to estimate the duration of star formation in forming GCs in a self-consistent manner. For comparison, we have also investigated models with a constant universal IMF. We have adopted a reasonable assumption that new stars can be formed from AGB ejecta which accumulates in the young GC. The basic parameter in this study is the initial mass of the GC-forming molecular cloud (MC; M_{mc}) and the lower cut-off mass of AGB stars ($m_{\text{agb},1}$) above which AGB ejecta can be used for secondary star formation. The principal results are as follows:

(1) The second generation (2G) of stars can be formed from AGB ejecta of the first generation (1G) of stars ≈ 30 Myr after the initial starburst of 1G stars within a GC in the fiducial model with $M_{\text{mc}} = 10^7 M_{\odot}$ and a non-universal IMF. However, the 2G star formation is truncated by SNe ≈ 16 Myr after the commencement of 2G star formation. This longer duration of 2G star formation results from the longer lifetimes of the most massive stars (i.e., lower $m_{\max} \approx 24 M_{\odot}$) in the model. This lower m_{\max} is due to the low SFR ($< 10^{-2} M_{\odot} \text{ yr}^{-1}$) in the 2G star formation from AGB ejecta. Star formation is inhibited for about 30 Myr until the last 2G SNII explodes.

(2) The third generation (3G) of stars are then formed from AGB ejecta of 1G stars ≈ 30 Myr after the truncation of 2G star formation in the fiducial model. This cycle of the formation of new stars and the abrupt truncation of star formation by SNe from the new massive stars in a forming GC can continue until the GC loses the intra-cluster gas by some physical processes, such as ram pressure stripping of the gas by the Galactic hot halo gas (e.g., Frank & Gisler 1976; Bekki 2006). The duration of star formation is longer for later generations of stars, because SFRs are lower (i.e., m_{\max} is lower) in the later generations such that the SNe explode after longer time scales. Thus, it is inevitable that forming GCs experience a number of star formation episodes each of which is separated by ≈ 30 Myr intervals.

Since chemical abundances of AGB ejecta depends on the masses of AGB stars, new stars formed from AGB ejecta can have different chemical abundances.

(3) The models with a constant canonical IMF also show multiple generations of stars during GC formation. However, the duration of each star formation episode is too short ($\approx 3 \times 10^6$ yr) because of the large number of SNe so that the total mass of these later generations of stars (M_{LG}) in a GC is quite small. For example, the total masses of 1G stars ($M_{1\text{G}}$) and all other generations of stars (e.g., 2G, 3G, and 4G) are $1.7 \times 10^6 M_{\odot}$ and $2 \times 10^3 M_{\odot}$, respectively, in the model with $M_{\text{mc}} = 10^7 M_{\odot}$. This result suggests that (i) M_{mc} of a GC-forming MC should be as large as $5 \times 10^8 M_{\odot}$ for the GC to have $M_{\text{LG}} = 10^5 M_{\odot}$ as observed for typical Galactic GCs with multiple stellar populations (e.g., C09) and (ii) almost all of the 1G stars need to be lost for the GC to have a high ratio of M_{LG} to $M_{1\text{G}}$. Since these two requirements appear to be very hard to be met, GC formation models with a universal IMF can be possibly ruled out.

(4) The present study predicts that low-mass GCs are unlikely to have *discrete* multiple stellar populations, even though they have 1G and 2G stellar populations. This is because m_{\max} during secondary star formation is lower than $9 M_{\odot}$ so that AGB ejecta can continue to be converted into new stars without being blown away by SNe. Accordingly, Na-O and Mg-Al anti-correlations between stars in these low-mass GCs should be continuous rather than discrete. We thus predict that more massive GCs are more likely to have discrete multiple stellar populations. This prediction will be assessed by future observations of chemical abundances of GCs with high-precision spectrograph.

(5) The present study suggests that massive star clusters with ages older than 10^7 yr can have no OB stars, even if they are currently forming new stars from AGB ejecta. This is mainly because m_{\max} is predicted to be significantly lower than $30 M_{\odot}$ owing to low SFRs in these clusters. Accordingly, the lack of OB stars in massive clusters with ages older than 10^7 yr does not necessarily mean the lack of secondary star formation in the clusters. Although massive clusters with secondary star formation only in low-mass and intermediate-mass stars can not show H α emission from OB stars, young stellar objects (YSOs with ages less than 1 Myr) or gas and dust (with the total masses being less than $10^4 M_{\odot}$) can be evidence for secondary star formation in these clusters. It is our future study to investigate whether LG stars can have different [Fe/H] from 1G stars in the present multiple burst scenario.

6 ACKNOWLEDGMENT

We are grateful to the referee for constructive and useful comments that improved this paper. KB, PK, and TJ acknowledge financial support through the DAAD (The Australia-Germany Joint Research Co-operation Scheme) throughout the course of this work. TJ was support by University of Bonn and by Charles University through a grant SVV-260441.

REFERENCES

- Banerjee, S., Kroupa, P., 2017, *A&A*, 597, 28
- Bastian, N., et al. 2010, *ARA&A* 48, 339
- Bastian, N., Cabrera-Ziri, I., Davies, B., Larsen, S. S., 2013, *MNRAS*, 436, 2852
- Bastian, N., Lamers, H. J. G. L. M., de Mink, S. E., et al. 2013, *MNRAS*, 436, 2398
- Bekki, K., 2007, *MNRAS*, 367, L24
- Bekki, K., 2011, *MNRAS*, 412, 2241 (B11)
- Bekki, K., 2013, 436, 2254
- Bekki, K., 2017a, *MNRAS*, 467, 1857 (B17a)
- Bekki, K., 2017b, *MNRAS*, 469, 2933 (B17b)
- Bekki, K., Norris, J. E., 2006, *ApJ*, 637, L109
- Bekki, K.; Campbell, S. W.; Lattanzio, J. C.; Norris, J. E., 2007, *MNRAS*, 377, 335 (B07)
- Bekki, K., Mackey, A. D., 2009, *MNRAS*, 394, 124
- Bekki, K., Yong, D., 2012, *MNRAS*, 419, 2063
- Bekki, K., Tsujimoto, T., 2016, *ApJ*, 831, 70
- Bekki, K., Tsujimoto, T., 2017, *ApJ*, in press
- Cabrera-Ziri, I., Bastian, N., Davies, B., Magris, G., Bruzual, G., Schweizer, F., 2014, *MNRAS*, 441, 2754
- Carretta, E., Bragaglia, A., Gratton, R. G., Lucatello, S., 2009, *A&A*, 505, 117 (C09)
- Carretta, E., Bragaglia, A., Gratton, R. G., Lucatello, S., D'Orazi, V., 2012, *ApJ*, 750, L14
- Carretta, E., 2014, *ApJ*, 795, L28 (C14)
- Conroy, C. & Spergel, D. N. 2011, *ApJ*, 726, 36
- D'Antona, F., & Caloi, V. 2004, *ApJ*, 611, 871
- D'Antona, F., Vesperini, E., D'Ercole, A., Ventura, P., Milone, A. P., Marino, A. F., & Tailo, M. 2016, *MNRAS*, 458, 2122
- Decressin, T., Meynet, G., Charbonnel, C., Prantzos, N. & Ekström, S. 2007, *A&A*, 464, 1029
- D'Ercole, A., Vesperini, E., D'Antona, F., McMillan, S. L. W., & Recchi, S. 2008, *MNRAS*, 391, 825 (D08)
- D'Ercole, A., D'Antona, F., Ventura, P., Vesperini, E., McMillan, S. L. W., 2010, *MNRAS*, 407, 854 (D10)
- Draine, B. T., Bertoldi, F., 1996, 468, 269
- Elmegreen, B. G., 2017, *ApJ*, 836, 80
- Fenner, Y., Campbell, S., Karakas, A. I., Lattanzio, J. C., Gibson, B. K., 2004, *MNRAS*, 353, 789
- Fontanot, F. De Lucia, G., Hirschmann, M., Bruzual, G., Charlot, S., Zibetti, S., 2017, *MNRAS*, 464, 3812
- For, B.Q., Bekki, K., 2017, *MNRAS*, 468, L11
- Frank, J., Gisler, G., 1976, *MNRAS*, 176, 533
- Gratton, R. G., Carretta E., 2010, *A&A* 521 54
- Gratton, Raffaele G.; Carretta, Eugenio; Bragaglia, A., 2012, *A&ARv*, 20, 50
- Goudfrooij, P., et al. 2014, *ApJ*, 797, 35
- Greggio, L., Rensini, A., 2011, *Stellar populations. A User Guide from Low to High Redshift*
- Hills, J. G., 235, 986
- Hsu, et al., 2013, *ApJ*, 764, 114,
- Karakas, A. I., 2010, *MNRAS*, 403, 1413
- Kirk, H., Meyers, P. C., 2011, *ApJ*, 64
- Kroupa, 2002, *Sci*, 295, 82
- Kroupa, P., Bouvier, J., 2003, *MNRAS*, 346, 369
- Kroupa, P., Weidner, C., Pflamm-Altenburg, J., Thies, I., Dabringhausen, J., Marks, M., Maschberger, T., 2013, *Planets, Stars and Stellar Systems Vol. 5*, by Oswalt, Terry D.; Gilmore, Gerard, Springer Science+Business Media Dordrecht, 2013, p. 115
- Larsen, S. S., et al. 2011, *A&A*, 532, 147
- Marks, M., Kroupa, P., 2012, *A&A*, 543, 8
- Marks, M., Kroupa, P., Dabringhausen, J., Pawlowski, M. S., 2012, *MNRAS*, 422, 2246
- Marino, A. F. et al. 2011, *A&A*, 532, 8
- Megeath, S. T., et al. 2016, *AJ*, 151, 5
- Milone, A. P., et al. 2013, *A&A*, 555, 143
- Milone, A. P., et al. 2017, *MNRAS*, 464, 3636
- Mucciarelli, A., Origlia, L., Ferraro, F. R., Pancino, E., 2009, *ApJ*, 695, L134
- Niederhofer, F., et al., 2016, *MNARS* in press (arXiv:1612.00400)
- Pfalzner, S., & Kaczmarek, T., 2013, *A&A*, 555, 135
- Pflamm-Altenburg, J., Kroupa, P., 2009, *MNRAS*, 397, 488
- Piotto, G., et al., 2005, 621, 777
- Ploekinger, S., Hensler, G., Recchi, S., Mitchell, N., Kroupa, P., 2014, *MNRAS*, 347, 3980
- Prantzos, N., Charbonnel, C., 2006, *A&A*, 458, 135
- Recchi, S., Kroupa, P., 2015, *MNRAS*, 446, 4168
- Ramirez Alegria, S., 2016, *A&A*, 588, 40
- Randriamanakoto, Z., et al. 2013, *APJ*, 775, L38
- Larson, R. B., 1998, *MNRAS*, 301, 569
- Renzini, A., et al., 2015, *MNRAS*, 454, 4197
- Renzini, A., Buzzoni, A., 1986, in *Spectral evolution of galaxies*, (Dordrecht, D. Reidel Publishing Co.), p.195
- Rossi, L. J.; Bekki, K.; Hurley, J. R. 2016, *MNRAS*, 462, 2861
- Salpeter, E. E., 1955, *ApJ*, 121, 161
- Smith, G. H., Norris, J., 1982, *ApJ*, 254, 594
- Stephens, I. W., et al. 2017, *ApJ*, 834, 94
- Testi, L., Palla, F., Natta, A., 1999, *A&A*, 342, 515
- Vazdekis, A., Casuso, E., Peletier, R. F., Beckman, J. E., 1996, *ApJS*, 106, 307
- Ventura, P., D'Antona, F., 2009, *A&A*, 499, 835
- Ventura, P., Carini, R., D'Antona, F., 2011, *MNRAS*, 415, 3865
- Ventura, P., et al. 2016, 831, L17
- Vesperini, E., McMillan, S. L. W., D'Antona, F., & D'Ercole, A. 2010, *ApJ*, 718, L112
- Weidemann, V., 2000, *A&A*, 363, 647
- Weidner, C., Kroupa, P., Larsen, S. S. 2004, *MNRAS*, 350, 1503
- Weidner, C., Kroupa, P., Pflamm-Altenburg, J., 2013, *MNRAS*, 434, 84
- Weidner, C., Kroupa, P., Pflamm-Altenburg, J., Vazdekis, A., 2013, *MNRAS*, 436, 3309
- Weidner, C., Kroupa, P., Pflamm-Altenburg, J., 2014, *MNRAS*, 441, 3348
- Yan, Z., Kroupa, K., Jeřábková, T., et al. 2017, submitted to *A&A*

APPENDIX A: CANONICAL AND TOP-HEAVY IMFS WITH MULTIPLE EPISODES OF STAR FORMATION

As discussed briefly in the main text, the duration of 2G star formation should be as short as 3×10^6 yr corresponding to the lifetime of the most massive star formed during the 2G formation in M1, if a canonical IMF is adopted. This means that the adopted continuous formation of SG stars without

being truncated by SNe is highly unrealistic. It is thus useful for the present study to investigate how the results of M1 can change if the truncation of star formation by SNe is self-consistently included for a canonical IMF. Here, star formation of LG populations (e.g., 2G, 3G etc) is truncated by the most massive SNe ($\approx 100M_\odot$) only ≈ 3 Myr after the start of the star formation in M9. The short duration of star formation in M9 is due to the adopted assumption of a canonical IMF with a fixed large upper mass cut-off.

Fig. A1 shows that the formation of discrete multiple stellar populations (1G-7G) is possible owing to the rapid cycle of star formation and its truncation by SNe. However, the duration of 1G-7G formation is so short that the total mass of new stars formed in each star formation episode is rather small ($< 10^3 M_\odot$). Consequently, the final M_{LG} is only $2.0 \times 10^3 M_\odot$, which is by almost three orders of magnitude smaller than M_{1G} . This means that 99.9% of 1G stars need to be preferentially lost in the later dynamical evolution of the GC for M_{LG} to be comparable to M_{1G} . This is the most serious version of the classic ‘mass-budget’ problem, which appears to be very hard to be solved.

If the IMF of 1G stars in a forming GC is top-heavy (e.g., Marks et al. 2012), then the total amount of AGB ejecta can be increased to some extent in the later formation phase of the GC. This can cause a difference in the later formation of stars from AGB ejecta. Fig. 10 describes the evolution of M10 in which the model parameters are exactly the same as those in M3 except for the IMF in the 1G formation ($\alpha = 1.35$ for 1G formation). The results are not so different from M3, which implies that the IMF slope in 1G formation is not so important in the formation of LG stars if the non-universal IMF is adopted for the LG formation. The top-heavy IMF can dramatically reduce the number fraction of low-mass long-lived stars ($0.1 \leq \frac{m}{M_\odot} \leq 0.8$). Therefore, the mass fraction of 2G low-mass stars to 1G ones can be significantly larger in M10 than in M3.

APPENDIX B: DEPENDENCE ON C_{sf}

Fig. B1 shows that the time evolution of SFR, M_g , and M_{gc} in M11 with a smaller C_{sf} ($=4.5$) is similar to that described for M2. However, the final mass of 1G stars in this model is only $9.0 \times 10^5 M_\odot$, which is less than 10% of the original gas mass. Therefore, the 1G stellar system is highly unlikely to be gravitationally bound after the removal of the left-over gas (e.g., Hills 1980). It is confirmed that the models with $C_{sf} \leq 4.5$ show such a low M_{1G} , which means that $C_{sf} \leq 4.5$ is not appropriate for a model of GC formation. The final total mass of LG stars in this model is also small ($M_{LG} = 1.7 \times 10^4 M_\odot$) owing to the smaller M_{1G} . We conclude that the adopted $C_{sf} = [9 - 18]$ is quite reasonable, not only because the star formation histories of 1G and LG in the models are consistent with those derived in hydrodynamical simulations of GC formation (B17b), but also because the formation of bound clusters is possible in the models.

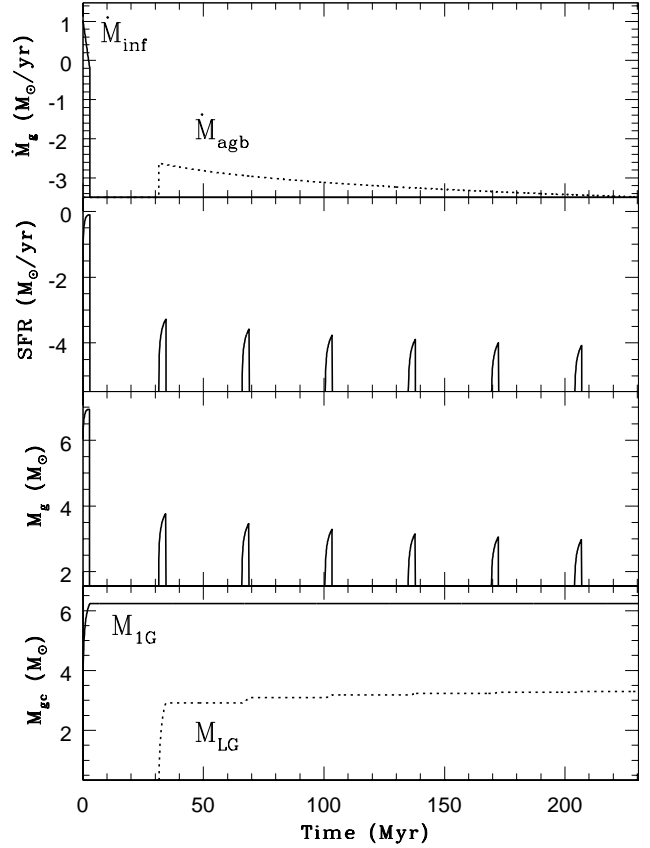


Figure A1. Time evolution of gas accretion (\dot{M}_{inf}) and AGB ejection rates (\dot{M}_{agb} ; top), SFR (second from top), total masses of stars in 1G and LG (second from bottom), and total gas mass (bottom) in M9.

APPENDIX C: APPLICATION OF THE IGIMF THEORY TO GC FORMATION

The simultaneous occurrence of a largely invariant IMF and a $m_{max} - M_{ecl}$ relation is most likely due to feedback self-regulation of the process of star formation on the molecular-cloud core scale (i.e., during the formation of an embedded cluster on a < 1 pc spatial scale and < 1 Myr time-scale, Kroupa et al. 2013). Remarkably, the form of this relation follows readily by a simple integration over the canonical IMF (e.g. Yan, Jeřábková & Kroupa 2017).

On the scale of whole closed star-forming systems (where closed star-forming system is one in which the star formation occurs within a self-regulated potential, a molecular cloud within a galaxy not being a closed star-forming system) such as galaxies, observations have shown the ensemble of freshly formed clusters to have a significant correlation between the mass in stars of the most massive embedded cluster and the system-wide SFR (Weidner et al. 2004; Randriamanakoto et al. 2013). This $M_{ecl,max} - SFR$ relation readily follows from an integral over the embedded cluster mass function (ECMF) subject to the mass being formed within about 10 Myr being the total mass in stars formed in the ensemble of ECs (e.g. Yan et al. 2017). Different self-regulated closed systems may form different ECMFs and the canonical assumption is that the power-law index of the ECMF, $\beta \approx 2$, i.e. essentially being the Salpeter index.

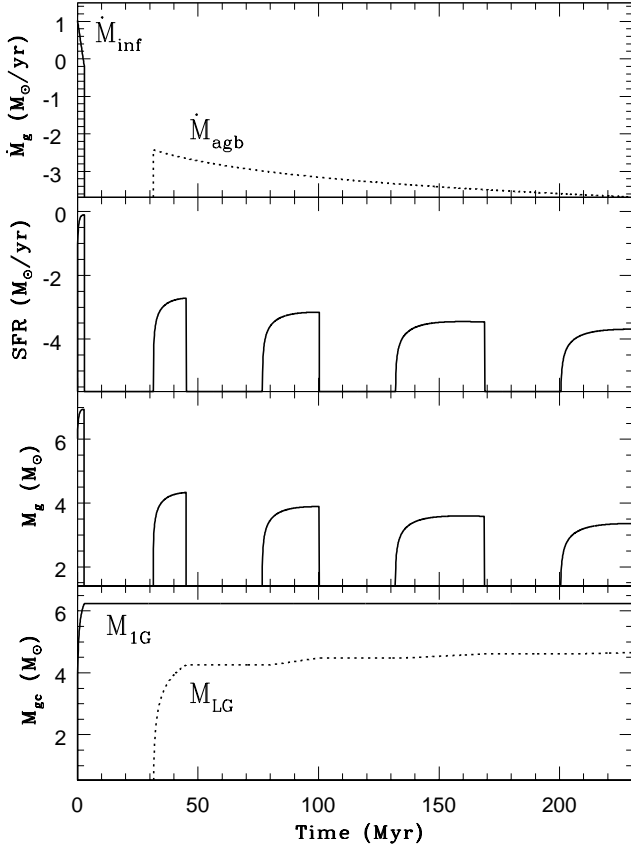


Figure A2. The same as A1 but for M10.

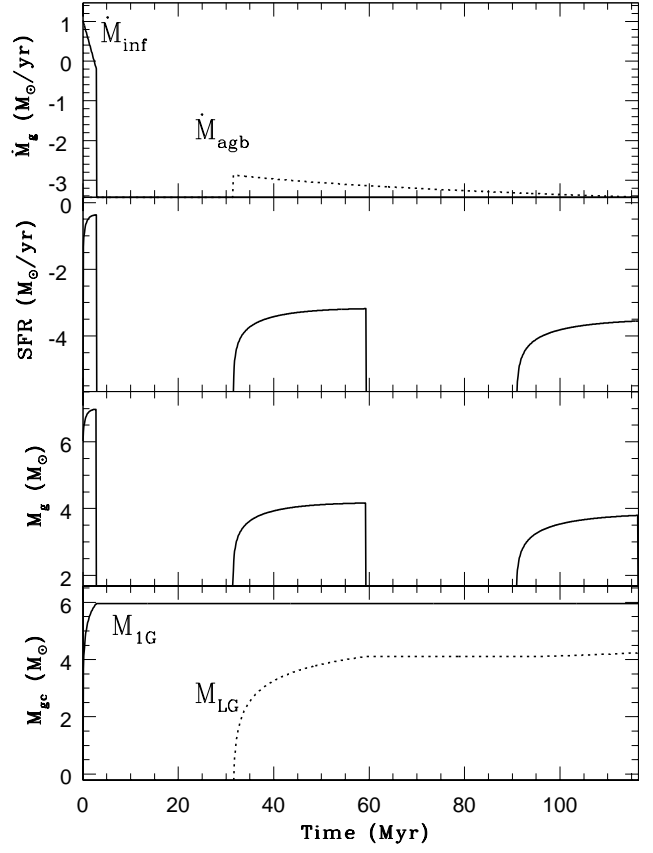


Figure B1. The same as A1 but for M11.

The combination of the $m_{\max} - M_{\text{ecl}}$ and the $M_{\text{ecl},\max} - SFR$ relations yields a $m_{\max} - SFR$ relation for the closed system (Yan et al. 2017): see also our Fig. 1.

In the context of the LG problem of GCs, the one-zone simulations presented here demonstrate that star-formation from AGB ejecta begins at a low level, because initially the molecular clouds need time to form and to buildup near the centre of the young GCs in which all SN events from the 1G have exploded. Thus, during the first about 1 Myr the embedded clusters will be low mass with a small m_{\max} . Their feeble feedback will cause the ISM which forms from the AGB ejecta to redistribute itself causing the formation of new embedded clusters within the inner region of the young GC. If the SFR of the closed system (the young GC) becomes sufficiently high, some massive stars may form and these may more strongly regulate further star formation. But over the time of about 10 Myr one may expect an ensemble of ECs to form, the most massive member of which will be limited by the SFR (i.e. by the amount of ISM mass available), just as in a galaxy.

It is emphasized here that the application of the IGIMF theory, as formulated elsewhere (e.g. Recchi & Kroupa 2015; Fontanot et al. 2017; Yan et al. 2017), has not been adjusted to produce a wanted result here, and that it is based purely on empirically deduced correlations. Also, application of the IGIMF theory to the scale of a young GC is merely an assumption made here which needs further testing. The assumption is thus that the IMF of the LG stars is not canon-

ical, but the non-canonical IMF is not adjusted arbitrarily but is defined by independently obtained empirical findings.